The Journal of Experimental Biology 210, 3395-3406
Published by The Company of Biologists 2007
doi:10.1242/jeb.007062

Uniform strain in broad muscles: active and passive effects of the twisted tendon of the spotted ratfish *Hydrolagus colliei*

Mason N. Dean[1,*], Emanuel Azizi[2] and Adam P. Summers[1]

[1]*Ecology and Evolutionary Biology, University of California Irvine, 321 Steinhaus Hall, Irvine CA 92697-2525, USA and* [2]*Department of Ecology & Evolutionary Biology, 80 Waterman Street, Box G-B, Brown University, Providence, RI 02912, USA*

*Author for correspondence (e-mail: mdean@uci.edu)

Accepted 12 July 2007

Summary

A muscle's force output depends on the range of lengths over which its fibers operate. Regional variation in fiber shortening during muscle contraction may translate into suboptimal force production if a subset of muscle fibers operates outside the plateau of the length–tension curve. Muscles with broad insertions and substantial shortening are particularly prone to heterogeneous strain patterns since fibers from different regions of the muscle vary in their moment arms, with fibers further from the joint exhibiting greater strains. In the present study, we describe a musculotendon morphology that serves to counteract the variation in moment arm and fiber strains that are inherent in broad muscles. The tendon of the anterior jaw adductor of the spotted ratfish *Hydrolagus colliei* is twisted such that the distal face of the muscle inserts more proximally than the proximal face. Using quantitative geometric models based on this natural morphology, we show that this inversion of insertion points serves to equalize strains across the muscle such that at any gape angle all fibers in the muscle are operating at similar positions on their length–tension curves. Manipulations of this geometric model show that the natural morphology is 'ideal' compared to other hypothetical morphologies for limiting fiber strain heterogeneity. The uniform strain patterns predicted for this morphology could increase active force production during jaw closing and also decrease passive resistance to jaw opening. This divergence from 'typical' tendon morphology in the jaw adductors of *H. colliei* may be particularly important given the demands for high force production in durophagy.

Key words: Chondricthyes, durophagy, modeling, jaw adductor, musculotendon complex.

Introduction

Tendons consist of several hierarchical levels of organization yet can often usefully be represented as simple tensile connections between muscle and bone. Indeed, many biomechanical analyses of force transmission necessitate treating a tendon as a single spring-like or tensile element (Goto et al., 2001; Herring et al., 1979; Peck et al., 2000; van der Helm and Veenbaas, 1991; van Eijden and Koolstra, 1998). However, this reduction ignores the fact that tendons usually have substantial thickness or breadth and therefore are more accurately characterized as many elements in parallel. Under some circumstances this aspect of tendon geometry may play a role in determining the tendon's biomechanical behavior (Goto et al., 2001).

The broader the tendon at its insertion the less it approximates a single linear tensile element and consequently, the greater the possibility of non-uniform mechanical behavior across the tendon during a muscle contraction. This becomes more obvious if we conceptually reduce a musculotendon complex (MTC, a muscle and its tendon) to a series of aligned linear tensile elements, and then separately consider the behavior of the two elements that are furthest apart (Fig. 1). If the element into which the MTC inserts (i.e. the bone) is hinged at one end and displaced by an antagonistic muscle, the MTC will exhibit strikingly different degrees of stretching across its body. As a result, the proximal and distal edges must shorten by different degrees to return the bone to its resting position (Fig. 1A,B). The breadth of an MTC's insertion can therefore result in a difference in the shortening patterns of its two faces (the two furthest edges of a broad muscle).

For a given joint excursion in a biological lever system, points further from the joint center of rotation experience greater fiber strains (length change per unit resting length) (Herring et al., 1979; Nordstrom and Yemm, 1974; Turkawski and van Eijden, 2001; van Eijden and Koolstra, 1998; van Eijden et al., 2002; Weijs et al., 1987). MTC width may then translate into an effect on whole muscle function: the broader an MTC, the more the moment arm varies between regions of the muscle. As active muscle tension is dictated by the degree of myofilament overlap (Gordon et al., 1966), and the degree of myofilament overlap is in turn determined by these differential moment arms, increased MTC width can translate into heterogeneous fiber strain and submaximal force production (Herring et al., 1979).

The detrimental effect of regional variation in moment arms

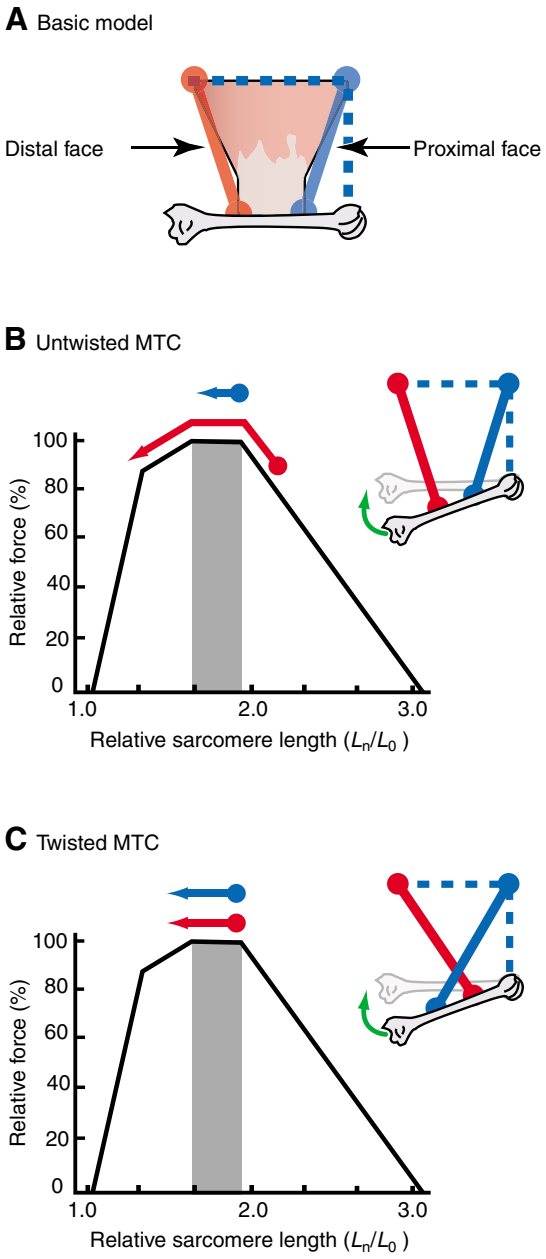

Fig. 1. Hypothetical mechanism for reduction of strain in a broad muscle. The anterior (red) and posterior (blue) margins of the muscle exhibit the most extreme strains, so we will consider these linear tensile elements as the boundaries of the parameter space (A). In a typical 'untwisted' morphology (B), the anterior face inserts furthest from the joint and therefore experiences greater strains, likely resulting in suboptimal force production (the region of optimal force production is indicated by the vertical gray bar in B and C). Conversely, in the 'twisted' conditions (C), the two faces undergo similar strains and therefore their force production capability is similar and high. The anterior/posterior coloring scheme used here is employed throughout the remainder of the figures. MTC, musculotendon complex.

can be counteracted by an anatomical change at different levels of organization. Resting sarcomere length and number, fiber length and activation times may all vary across the muscle such that fibers on opposite edges of the muscle might still perform optimally despite wide variation in strain (e.g. Herring et al., 1979; Nordstrom et al., 1974; Turkawski and van Eijden, 2001; van Eijden et al., 2002). In theory, a solution to heterogeneous strains might also be reached at the level of whole muscle geometry by relocating the insertion points relative to the joint (Fig. 1C). Fiber strain increases with distance from the joint; therefore moving the proximal face insertion distally increases its strain to match that of the contralateral face. The differences in fiber strain between the faces should decrease as the distal face insertion moves closer to the joint and the proximal face insertion moves farther away. Based on these differences, we hypothesize that an inversion of insertion points (where the distal face inserts closer to the joint than the proximal face) would alleviate the detrimental effects of tendon width in broad muscles (Fig. 1C). This hypothetical 'twisted' tendon would provide a geometric solution to the problem of unequal strains, potentially maximizing force output in broad MTCs.

In this study, we describe a natural example of this theoretical morphology, where the inversion of insertion points may function to equalize fiber strain. This gross morphological alteration to the 'typical' tendon is exhibited in the anterior jaw adductor (AMA-α) of the spotted ratfish *Hydrolagus colliei* (Chondrichthyes: Holocephalii). Unlike the two more posterior jaw adductors, the tendon of the AMA-α inverts, twisting 180° about its longitudinal axis before inserting on the mandible (Fig. 2). As a result, the posterior face of the muscle inserts more anteriorly than the anterior face and the portion of the tendon that is medial at the muscle–tendon junction is directed laterally at its insertion.

The musculoskeletal anatomy of this species is therefore a natural system for testing our theoretical model. We hypothesize that the inversion of moment arms caused by the twisted tendon morphology of the AMA-α of *H. colliei* equalizes strain throughout the muscle. We use a quantitative geometric model based on the cranial anatomy of *H. colliei* to predict strain patterns experienced by the jaw adductors during feeding and through morphological simulations, examine the effect of a twisted tendon and alterations in musculoskeletal geometry on variation in muscle strain patterns. We also characterize the development of this morphological character across an ontogenetic series of *H. colliei*.

Materials and methods

Animals and anatomy

Hydrolagus colliei Lay and Bennet 1839 is a demersal, cold-water cartilaginous fish. It is a durophagous benthic grazer and is believed to sift through the sediment for molluscs, echinoderms and crustaceans (Didier, 1995; Ebert, 2003; Johnson and Horton, 1972). The three adult male *H. colliei* (440–500 mm total length, *TL*) used in this study were collected by trawl off the San Juan Islands, Washington, and euthanized with MS-222 solution following a separate study on *H. colliei* jaw mechanics and bite force (D. R. Huber, M.N.D. and A.P.S., manuscript in preparation) (Huber et al., 2004). The skin on the left side of the head was removed to expose the three jaw adductor divisions (Fig. 2). Identification of these divisions is based, with slight modification, on Didier (Didier, 1995).

To determine the ontogenetic trajectory of this character we also dissected the right cheeks of five museum specimens

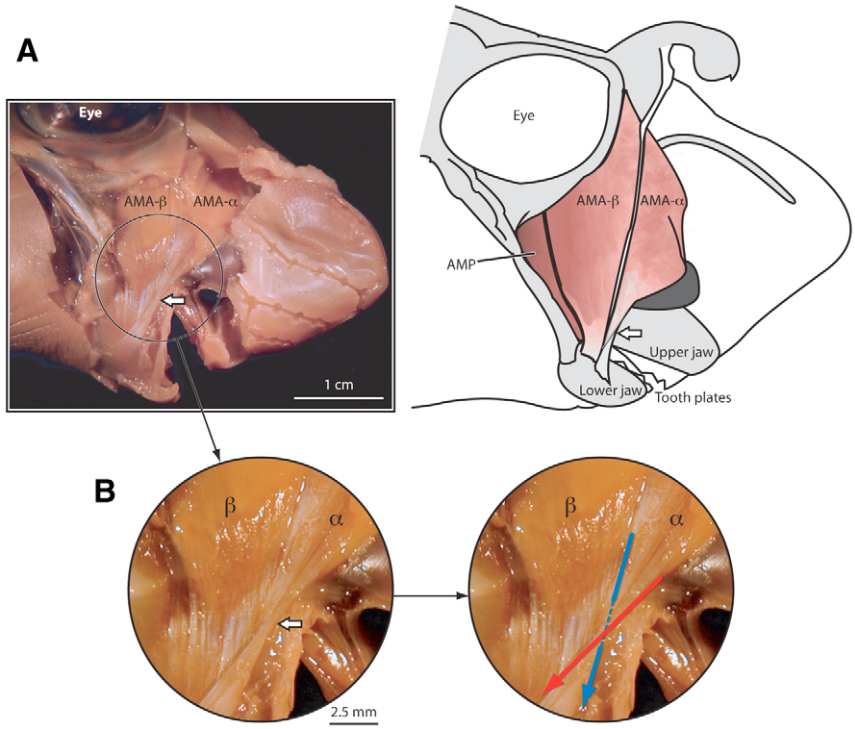

Fig. 2. Morphology of the cranial musculature in the head of the spotted ratfish *Hydrolagus colliei*. (A) The schematic on the right illustrates the musculature labeled on the left. (B) The twisted portion of the tendon (circled) expanded. Although all three adductors insert on the lower jaw, only the anterior adductor (AMA-α) exhibits a pronounced twist in its tendon (its approximate middle indicated throughout the figure by a white arrow) where the anterior face (red arrow) inserts more posteriorly than the posterior face (blue arrow). The *Hydrolagus* schematic shown here is used in the remainder of the figures with the anterior jaw adductor isolated for clarity. AMA-β, posterior division of the anterior adductor mandibula; AMP, adductor mandibula posterior.

(Scripps Marine Vertebrate Collection, La Jolla, CA, USA), representing sizes ranging from recently hatched animals to adults. The AMA-α tendons of these specimens were compared qualitatively to clarify whether the tendon is twisted at all ontogenetic stages.

We examined the following male specimens: SIO68-90 (~100 mm *TL*); SIO60 439-5A (~114 mm *TL*); SIO93-44 (~157 mm *TL*); SIO80-109 (~196 mm *TL*); SIO80-109 (~273 mm *TL*).

Geometric model

We constructed a geometric model of a hypothetical jaw adductor and applied it to the AMA-α in order to simplify and quantitatively characterize the morphology of the muscle (Fig. 3; Appendix). The model reduces the muscle to a simple shape composed of four lines: the origin line ($\overline{AE}$), the insertion line ($\overline{EF}$), the anterior muscle face (extending from point A) and the posterior face (extending from point B).

The lengths of the anterior and posterior faces of an MTC can be calculated at any gape angle (i.e. degree of rotation of the insertion line) and compared with resting MTC length in order to determine a percentage length change (strain) of the two faces of the muscle. Strain homogeneity can then be calculated as the difference in strain between the two faces (ΔS), with zero representing uniform strain in the muscle and positive and negative values indicating relatively higher and lower anterior face strains, respectively (Fig. 4).

Model simulations

Twisted tendon vs untwisted tendon

This geometric model allows us to manipulate MTC geometry (e.g. by adjusting insertion locations, MTC lengths, etc.) and make quantitative prediction of the effect of morphology on muscle strain. For example, we can make a simplified comparison of twisted and untwisted tendon morphologies by altering the configuration of the anterior and posterior faces of the simulated muscle in our geometric model. In a muscle with an untwisted tendon, the muscle faces do not interact and the shape is delimited by the lines $\overline{AB}$, $\overline{BE}$, $\overline{EF}$ and $\overline{AF}$ (Fig. 3). However, in a muscle with a twisted tendon, the anterior and posterior faces cross and $\overline{AB}$, $\overline{BF}$, $\overline{EF}$ and $\overline{AE}$ represent the schematic muscle (Fig. 3).

The *x*,*y* coordinates of the seven landmarks were determined from a digital photograph of dissected animals using Image J v. 1.2 (National Institute of Health, Bethesda, MD, USA). We calculated the lengths of the two faces of the muscle for twisted and untwisted conditions at gape angles from 0° to the natural maximum gape angle of 40° in 2° increments. These values were then divided by resting MTC lengths (L_r) at a gape angle of 0° to give muscle fiber strains for anterior and posterior faces of jaw adductors with twisted and untwisted tendons. Regional strain differences (ΔS) could then be compared across gape angles to determine whether one system was more effective at strain homogenization.

Our models maintain the same origin and insertion points between twisted and untwisted systems, meaning that muscle faces in the twisted system insert at a shallower angle than those in the untwisted system (e.g. compare the slopes of the anterior faces of the two conditions in Fig. 3). The closer the insertion angle is to 90°, the greater the contribution of contractile force to bite force; we define the perpendicular component of muscle force as ‘effective force’ and calculate this variable using the sines of the insertion angles (see Appendix). We then compare the effective force in each face of the MTC to compare the proportion of force transmitted to a bite in the twisted and untwisted condition.

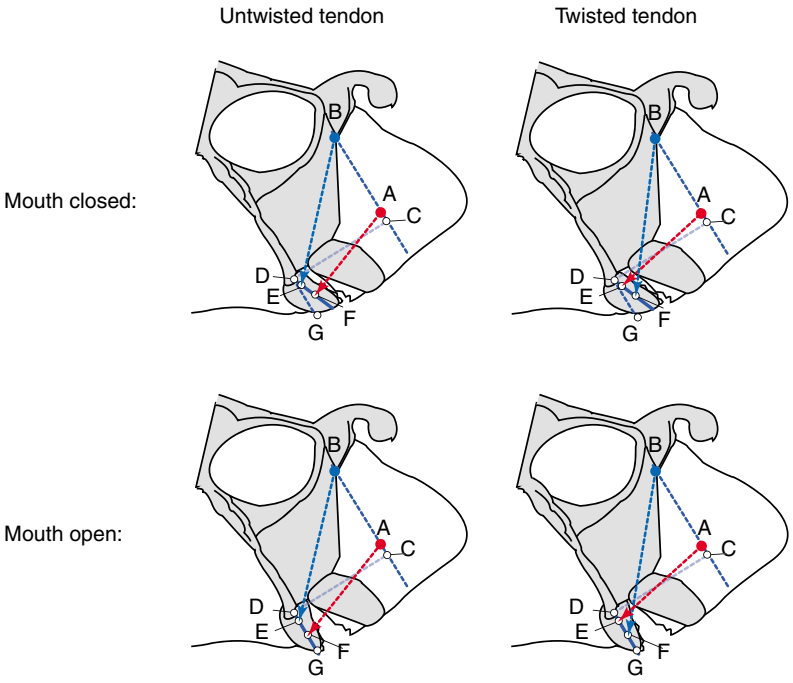

Fig. 3. Geometric model of the anterior division of the adductor mandibula of the ratfish. The model can be easily adjusted to represent the twisted and untwisted conditions by changing the insertion points of the anterior and posterior faces (see Appendix). We examined the effect of gape angle on strain, in both twisted and untwisted conditions, by calculating the lengths of the anterior and posterior muscle faces at gape angles from 0–40°.

Twisted tendon geometric manipulations

In our second manipulation, we altered individual length variables in the twisted tendon model using an iterative script written for MATLAB v.14 (The MathWorks, Inc., Natick, MA, USA) based on our geometric model. We chose four variables related to the location and width of the muscle attachments: interorigin width ($\overline{AB}$), interinsertion width ($\overline{EF}$), muscle length ($\overline{CD}$), and distance of the posterior insertion from the jaw joint ($\overline{DE}$). By altering the length of one variable at a time and observing the effect on ΔS, we were able to determine the relative importance of specific geometric factors to the system. The strain pattern within the muscle was calculated at a minimum value for each variable and across gape angles from 0° to 40° (in 2° increments). The variable was then increased by increments of 1 mm to an arbitrary maximum (usually approximately two times the length of the animal's natural morphology) and at each length we calculated strain homogeneity across the same gape range. For each variable the animal's natural geometry lay approximately in the middle of the range of simulated lengths.

Each iterative geometric manipulation was calculated for an MTC that was only 24.5% muscle (the average value for the natural morphology; see Appendix) and an MTC that was 100% muscle. These two conditions allowed us to explore the effects on predicted strains of variation in the proportion of MTC that is muscle. The former condition accounts for the underestimation of muscle strains in MTCs that are not entirely muscle (see Appendix) and likely gives a more accurate picture of strains experienced by the contractile elements. The latter condition models strains applied to the entire MTC, and assumes a muscular insertion.

These iterations resulted in a topographic functional landscape with gape angle on the *x*-axis, variable length on the *y*-axis and ΔS on the *z*-axis. Strain homogeneity was therefore illustrated in those regions of the graph where the *z*-axis term was zero. By locating the animal's natural morphology (i.e. the observed length for a given variable) relative to regions of strain homogeneity in this landscape, we could determine how closely the animal's morphology approximates the optimal geometry for strain homogenization.

Results

Morphology

In adults, the anterior adductor mandibulae muscle appears to be comprised of white (glycolytic) fibers and has two divisions, AMA-α and AMA-β, both of which originate anterior to the orbit. The latter division inserts more closely to the jaw joint. The posterior adductor mandibulae division, AMP, originates posteroinferior to the orbit and shares an insertion with the AMA-β. This division appears to be composed entirely of red (oxidative) muscle fibers (Fig. 2).

The AMA-α is roughly trapezoidal in shape with a broad ethmoidal origin that tapers considerably to a narrow tendinous insertion on the jaw. The tendon of the AMA-α is considerably wider and longer than the tendons of the other two divisions and twists about its longitudinal axis such that its medial face faces laterally at its insertion. In lateral view, the muscle fiber length/tendon length ratio is relatively uniform across the muscle, although the posterior regions are slightly (~5%) more tendinous. The AMA-α MTC has a much larger proportion of tendon than the other two adductor divisions: the former is only 23.0–27.0% muscle, whereas the MTCs of the AMA-β and AMP are both more than 50% muscle. The tendons of the two posterior divisions exhibit no twisting and insert directly on the jaw (Fig. 2).

The twist of the AMA-α tendon in *H. colliei* was present for all size classes observed (97–500 mm *TL*), yet becomes more pronounced with age. In the youngest animal (97 mm *TL*), the twist is established at its insertion on the mandible, but the anterior margin of the remainder of the tendon is only loosely folded caudally, such that it can be 'unrolled' with minimal pressure from forceps. With age, the twist extends dorsally and a greater proportion of the tendon exhibits the twist. In animals >196 mm *TL*, the twist is firmly defined and cannot be 'unrolled'.

Twisted tendon vs untwisted tendon

MTCs with untwisted tendons exhibit more extreme absolute strains than those with twisted tendons (Fig. 4A) and, as expected, both systems show an increase in absolute MTC strain with gape angle. For the purpose of this discussion, we will refer to the more extreme case where the MTC consists of 24.5% muscle; the same trends hold for the 100%-muscle MTC, only

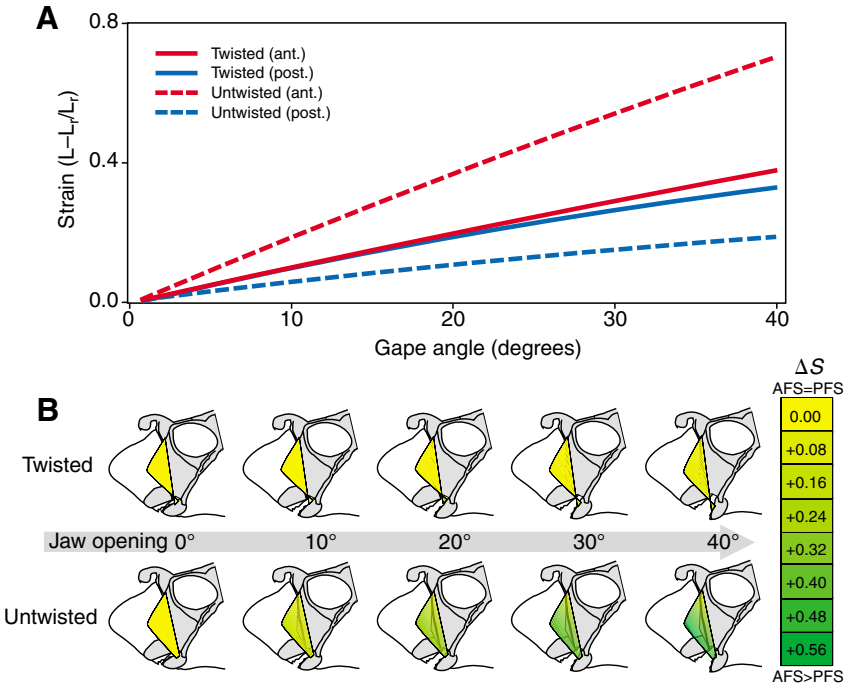

Fig. 4. (A) The effect of gape angle and tendon morphology on muscle strain in the anterior division of the adductor mandibula of the ratfish. In the untwisted condition (broken lines), strain increases much more rapidly in the anterior face (red line) than the posterior face (blue line) as the mouth is opened to maximum gape (~40°). As a result, at maximum gape, there exists more than a 50% difference in strain between the faces of the muscle (relative to their respective resting lengths). This is an order of magnitude difference over what is seen in the twisted condition, where the strain differences in the two faces are never more than 5.5%. These results are represented schematically in (B) where strain differences (ΔS) between the anterior and posterior faces of the muscle in each condition (twisted and untwisted) are colored in a gradient from yellow (equal strains) to green (an anterior face strain that is greater by 56% of resting length). AFS, anterior face strain; PFS, posterior face strain.

the magnitude of the differences is less. At maximum natural gape (~40°) and assuming no stretch of the tendon during muscular contraction, the anterior face of the untwisted MTC must shorten by 71.5% of its resting length to close the mouth, while the posterior face of the MTC must shorten by only 18.8% of its resting length. In contrast, the two faces of the twisted tendon system exhibit intermediate strains; for example, the strain of the anterior face of the twisted MTC system is approximately half of that of the anterior face of the untwisted system at maximum natural gape. The strains of the two faces of the MTC in the twisted tendon system are also approximately equal at all gapes, with ΔS never exceeding 0.049 between gape angles of 0° and 40°. In other words, during a normal gape cycle the strains in the two contralateral regions of the MTC never differed by more than 4.9% of resting length.

These relationships are highlighted in a plot of ΔS for the two morphologies (Fig. 4B). Across a natural gape cycle, the ΔS for the twisted tendon approximated zero, indicating uniform fiber strain across the muscle. In the untwisted system, however, ΔS continued to increase to a 52.7% difference between the two faces at the maximum natural gape.

At smaller gape angles and given the same insertion points, the twisted tendon results in a detriment to bite force production as compared to the untwisted condition (Fig. 5). This is evidenced by the shallower insertion angles of both faces of the twisted MTC relative to the untwisted MTC, resulting in a lower effective force (i.e. a smaller value for the sine of the insertion angle). When the mouth is closed (0° gape), the anterior face of the untwisted MTC inserts at an angle approximating 90°, meaning that contractile force is nearly in line with bite force and the majority of contractile force contributes to bite force (Fig. 5, red lines). The anterior face of the untwisted MTC exceeds a 90° insertion angle immediately after mouth opening, resulting in increasingly less effective force transfer as the gape widens. The anterior face of the twisted MTC reaches a 90° insertion angle at approximately a 10° gape, meaning that, unlike an untwisted MTC, its force transfer is more efficient with the mouth open than closed. The anterior face of the twisted system continues to be more efficient than that of the untwisted system for the remainder of the gape cycle.

The resting insertion angles of the posterior faces in both conditions are less than 90° and decrease with increasing gape angle meaning that full force potential (i.e. 90°) is never reached in the posterior faces of the MTCs (Fig. 5, blue lines). At all gape angles, the posterior face of the twisted system has a shallower insertion angle than that of the untwisted system and therefore always has a lower effective force.

At gape angles of less than approximately 10°, the shallow insertion angles of both faces of the twisted MTC result in a lower effective force than that of the untwisted system (Fig. 5, black lines). However, the higher effective force of the anterior face of the twisted MTC at larger gape angles eventually results in an equality of average effective forces for the two systems at gape angles greater than approximately 20°.

Twisted tendon geometric manipulations

Our geometric simulations created functional and morphological landscapes in which the *x*-axis (gape angle) and *y*-axis (morphological variable length) represent animal anatomy and the graph's elevation (*z*-axis) depicts strain homogeneity. These simulations allow us to visualize the effects of hypothetical anatomies on strains in the anterior jaw adductor of *H. colliei*. By localizing regions of the graph where the *z*-term, ΔS, equaled zero, we pinpointed morphologies that permit uniform fiber strain across the muscle.

For all four variables, and across a range of natural gape angles, the morphology of *H. colliei* consistently inhabited a region characterized by little variation in strain (Fig. 6; two morphological manipulations are presented as examples). The

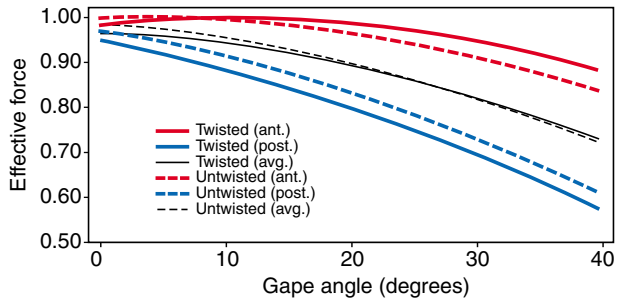

Fig. 5. The effect of insertion angle on the proportion of contractile force in the direction of bite force (effective force). Insertion angles closer to 90° exert 100% of their force normal to the jaw (in the same direction as bite force) and therefore have an effective force of 1.0. The twisted and untwisted conditions are modeled using the same insertion points and therefore have the same in-lever moment arms; however, the twisting of the tendon results in shallower insertion angles and therefore a lower resting effective force. As gape increases from 0 to 40°, insertion angle increases for the anterior face and decreases for the posterior face of both conditions. Because the anterior face of the twisted condition has a resting insertion angle of less than 90°, its effective force is highest at a gape of approximately 10°. Although the posterior face of the twisted system is always less efficient than its untwisted counterpart, its anterior face remains more efficient than the untwisted anterior face for larger gapes, resulting in an eventual equality of average effective force for both conditions. Ant., anterior; Post., posterior; Avg., average.

natural morphology resulted in less than 1.5% difference in strain between the two muscle faces ($|z|<0.015$) when accounting for tendon length and less than 0.5% difference in strain ($|z|<0.005$) when considering the entire MTC. This strain homogeneity plateau ($|z|<0.05$) narrowed (i.e. spanned less y-axis distance) considerably with increasing gape angle, illustrating that at smaller gape angles strain differences are low regardless of morphology.

Strain heterogeneity increased more rapidly with changing morphology when tendon length was considered, as revealed by the steeper z-axis gradients in Fig. 6A,B. Although the shape of the strain homogeneity plateau was similar between manipulations that do and do not consider tendon length, the plateau is smaller and narrower in the former condition. Therefore, as the proportion of tendon in an MTC increases, a narrower range of morphologies homogenize strain across gape angles from 0 to 40°.

Discussion

Our model suggests that twisting the tendon of a broad MTC promotes uniform strain across the face of the muscle. Heterogeneous fiber strain is an inherent property of broad muscles attached to rotating structures and is the result of the differential excursion of widely spaced insertion points and the difference in the length of their moment arms. A twisted tendon counteracts regional variation in muscle moment arms such that a given gape angle produces similar fiber strains at either face of the muscle.

Muscle strain affects both active and passive force production. As myofilament interaction determines active tension, all muscle fibers have a length range over which optimal active force production is possible (the plateau in a length–tension curve) with active tension decreasing at lengths longer and shorter than the optimum (Gordon et al., 1966; Herring et al., 1979). Passive force, however, is dictated by parallel and series elastic elements in the MTC and increases exponentially beyond the muscle length corresponding to the optimal plateau of the length–tension curve (Peck et al., 2000; Winter, 1990; Woittiez et al., 1983). If we assume that the optimum sarcomere length is the same throughout the muscle (Herring et al., 1979), two fibers (and their sarcomeres) subjected to different strains (i.e. at a given jaw angle) will likely function at different positions along the length–tension curve, resulting in differential force production (Gillis et al., 2005; Nordstrom et al., 1974). We posit that twisting the tendon allows anterior and posterior muscle fibers to operate in similar regions of their length–tension curves, which may result in decreased passive resistance during jaw opening and enhanced active force production during jaw closing (Fig. 7).

Passive effects: jaw opening

Opening the jaw increases passive tension in the jaw adductors as they are stretched. In an untwisted system, the degree of stretching may vary considerably across the muscle due to the distance between insertion points, as points further from the jaw joint undergo greater excursions during jaw opening (Goto et al., 2001; Herring et al., 1979; Pappas et al., 2002; van Eijden and Turkawski, 2001). Anterior fibers in the hypothetical untwisted system of the *H. colliei* AMA-α are predicted to undergo strains that are 50% larger than posterior fibers (relative to their respective resting lengths) at maximum gape (Fig. 4). Similarly, fibers in pig masseter muscle elongate over 50% of resting length compared to 13% in posterior fibers (Herring et al., 1979). As the gape widens, there is a progressive increase in the contribution of the anterior muscle region to passive force production as anterior fibers lengthen faster and begin to climb the exponential slope of the passive force curve well before posterior fibers (van Eijden et al., 2002). The resultant increase in passive force may provide some assistance in generation of an adductive moment, especially at the start of the closing phase when the jaw abductors are first inactivated and stored energy is released from elastic elements (Nordstrom et al., 1974; van Eijden et al., 2002). This is likely more useful in generating fast closing movements rather than forceful ones.

Twisting the tendon reduces the high passive forces predicted for the anterior portion of the MTC. Because both faces undergo similar strains at any given gape angle, anterior and posterior fibers both operate on a region of the length–tension curve where passive forces are low. Passive forces do not increase as fast in this system and the rate of length change is reduced in the anterior fibers. This mitigation of anterior passive tension for any gape angle translates to an overall reduction in passive forces in the twisted system as compared to the untwisted system. As a result, there is likely less resistance to jaw opening in a twisted system (Koolstra and van Eijden, 1997), which may decrease the muscular work associated with jaw opening and allow for a larger range of gapes.

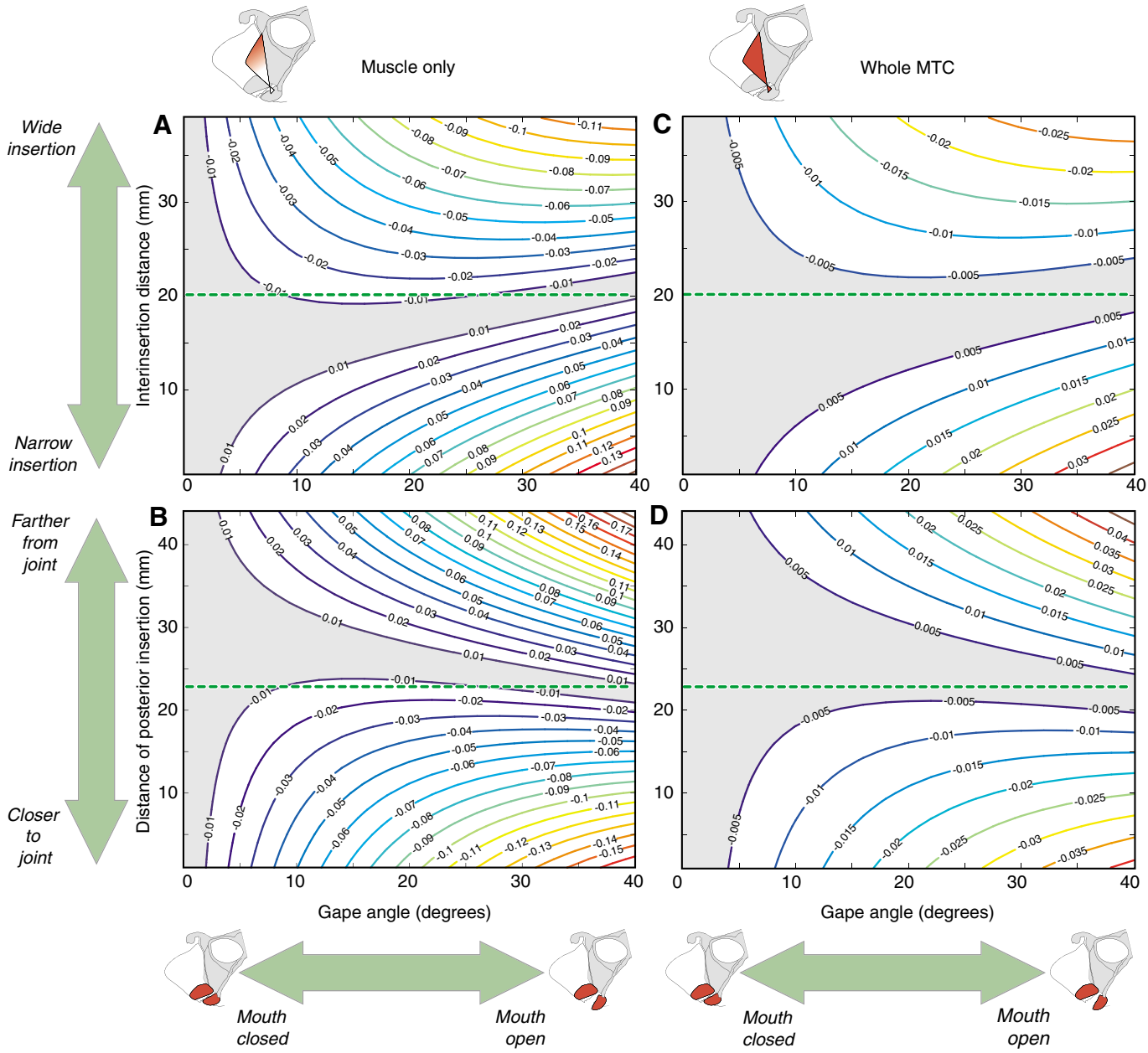

Fig. 6. The effect of gape angle and adductor mandibula geometry on regional strain variation (ΔS). In all panels, gape angle is on the *x*-axis, theoretical manipulations of morphology are on the *y*-axis and ΔS is on the *z*-axis. (A,B) Strain fields resulting from an MTC that is 24.5% muscle and (C,D) an MTC that is 100% muscle. (A,C) Modifications in the width of the muscle insertion; (B,D) the distance of the posterior insertion of muscle from the jaw joint. *z*-axis variables represent strain differences (ΔS) between the anterior and posterior faces of the muscle, forming a topographic representation of strain heterogeneity. The shaded plateau region of each graph indicates morphologies where strains in the anterior and posterior muscle faces are nearly similar (±1.0% ΔS in A,B; ±0.5% ΔS in C,D). The broken green line represents natural morphology/geometry of the adductor mandibula of the ratfish. This natural morphology generally corresponds to regions of low strain variation across a broad range of gape angles.

Active effects: jaw closing

The force produced during jaw closure is determined by the active tension generated in the jaw adductor muscles. The strain in muscle fibers at maximum gape determines the point on the length–tension curve where these fibers are operating at the start of jaw closing. As a result, in an untwisted system where fiber strains are heterogeneous across the muscle, the force production capabilities of anterior and posterior fibers may be very different at any gape angle. Indeed, the differential sarcomere lengthening in the masseter of the pig during jaw opening is largely a consequence of the geometry of the muscle and its attachments (Herring et al., 1979). Anterior fibers will undergo larger strains than posterior fibers and (again assuming homogeneous sarcomere lengths) will tend to reach their optimal force plateau at smaller gapes during jaw closing. This would broaden the range of gapes over which intermediate forces are generated, since at any closing gape angle some portion of the muscle is likely operating at or near peak force production (Goto et al., 2001;

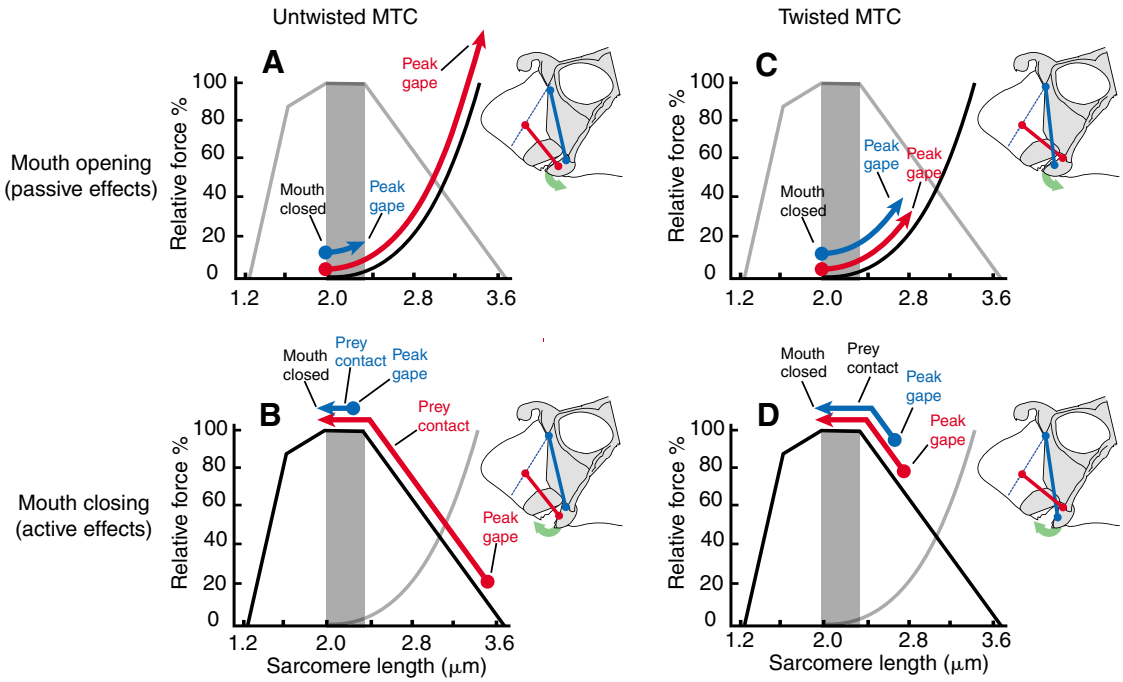

Fig. 7. The effect of sarcomere length and tendon morphology on active and passive force production in the anterior division of the adductor mandibula of the ratfish. Sarcomere length is estimated from predicted muscle strains during jaw opening (see Fig. 5) and a resting length of 2.0 μm. In the untwisted condition (A,B), passive tension increases more rapidly in the anterior face than in the posterior face as the jaw is opened (A). This results in the two portions of the muscle beginning their active tension generation at disparate points on their active curves (B) and having heterogeneous force production capabilities, lowering the whole muscle force output at prey contact. In contrast, the faces of the muscle in the twisted condition (C,D) occupy similar portions on both their active (D) and passive (C) tension curves, allowing more optimal active tension generation and a wider gape without the detrimental effects of high passive tension forces.

Herring et al., 1979; Pappas et al., 2002; Turkawski and van Eijden, 2001; van Eijden and Koolstra, 1998; van Eijden et al., 1997). A similar pattern has been illustrated in opossums, which employ multiple jaw adductor muscles with different lines of action such that each muscle is most effective at a different gape (Weijs et al., 1987). As a result, force is consistent across a wide range of gape angles but the contribution of individual muscles to bite force varies with jaw position.

Instantaneous whole muscle active tension is a summation of the forces generated by all regions of the muscle; in a jaw adductor, maximum force occurs at gapes where the majority of fibers occupy their optimal force plateau. At larger gapes in an untwisted system, posterior fibers contribute most to active force while overstretched anterior fibers produce active force well below their optimum (Figs 4, 7). This trade-off of anterior–posterior force production means that even when anterior fibers are overextended at large gapes, posterior fibers can still produce high tensions (Nordstrom and Yemm, 1974). It could be predicted then that forces would decrease at smaller gape angles as an increasing number of the posterior fibers shorten past their optimal length (i.e. slip off their force plateau); in rabbits, forces are higher (60–100% L_0 or maximum force) at larger gapes than at occlusion (20–60% L_0) (Turkawski and van Eijden, 2001). Intermediate gapes/lengths are therefore likely to maximize force production as the center of the muscle may be recruited maximally while the extreme faces are not far removed from their force optima. This is supported by studies on rats showing that at the gape angle for maximum force production, anterior and posterior fibers are longer and shorter than optimal length, respectively (Nordstrom and Yemm, 1974). Other mammalian studies have determined maximum active tension to be generated at gapes between ~10° and 20° (Turkawski and van Eijden, 2001; van Eijden et al., 1997).

In a twisted system, anterior and posterior fibers occupy similar places on their active tension curves (Fig. 7). We can assume, due to the calculated homogeneous strains, that optimal force is generated at the same gape for both faces (Fig. 7). In contrast to the untwisted condition this would allow for higher peak forces produced over a narrower range of gapes. Twisting of the tendon therefore optimizes a broad muscle for force production by homogenizing fascicle strain such that the majority of fibers reach their length–tension plateau at similar gapes.

Although twisting of the tendon allows the muscle to function largely at its optimal strain, the resulting decrease in insertion angle relative to a parallel fibered muscle with a similar width insertion may compromise some of the overall force actually transmitted to the bite (Fig. 5). However, our simulations show that this decrement in force is small (Fig. 5). The contribution of contractile force to bite force (effective force) of the anterior face of the twisted MTC exceeds that of the anterior face of the untwisted system for gapes larger than 10°. On average the contribution of contractile force to bite force is essentially the same for both systems at larger gape angles where the animal is likely crushing prey (see below). The detrimental effects of shallow insertion angle become more pronounced with wider MTCs with twisted tendons; yet as whole muscle contractile

force is a function of cross-sectional area, these disadvantages can be counteracted by concentrating muscle tissue in the middle of the muscle where the ~90° insertion angle ensures efficient force transfer.

The force production mode of the twisted MTC (high forces produced over a limited gape range) is well suited to eating hard prey. Soft-tissue carnivory necessitates shearing and force generation over a range of gapes, whereas durophagy hinges on a single force production event where the jaw adductors generate enough isometric force to cause failure of the prey's exoskeleton (Korff and Wainwright, 2004; Wainwright, 1987). The twisted tendon of the AMA-α of *H. colliei* suggests that there is a narrow range of gapes over which a majority of the muscle is generating peak force simultaneously. This may approximate the gape at which the mineralized tooth plates contact the prey; at that point, the prey item will not deform and forces will increase quickly as the muscle contracts isometrically. The muscular morphology and physiology of the ratfish suggests a pronounced crushing event causing catastrophic failure of the prey exoskeleton; although *H. colliei* exhibits the highest recorded mass-specific bite force of any chondricthyan fish, its adductor musculature has been shown to fatigue significantly faster than that of a piscivorous shark, *Squalus acanthias* (Huber et al., 2004).

Ontogeny and epigenetic factors

Our examination of the effects of hypothetical morphologies on intramuscular strains in *H. colliei* illustrates that the adult MTC anatomy/geometry approximates an optimal morphology for uniform strain. This MTC geometry (the twist in the anterior adductor tendon), however, is not fully established at parturition but develops during ontogeny. The apparent 'tuning' of the system to the functional demands of the feeding mechanism (Fig. 6) suggests that tendon remodeling is in response to epigenetic cues. We hypothesize that the triggers are mechanical and that remodeling of the tendon is in response to the potentially damaging stresses of durophagy.

The benefits of a twisted tendon on active and passive aspects of the length–tension curve (see above), though seemingly incongruent, may be related through the ecology of the ratfish. Development of a twist in the anterior jaw adductor as the animal grows would allow a larger gape (passive effect) and therefore the ability to eat larger prey. *Hydrolagus colliei* are durophagous at all examined ontogenetic stages (Ebert, 2003; Johnson and Horton, 1972); if mean prey size increases with ratfish size then this illustrates the concomitant importance of maximal force production (active effects) as larger gastropods require more crushing force (Hernandez and Motta, 1997; Korff and Wainwright, 2004; Wainwright, 1987). A diet containing increasingly harder prey is supported by the fact that older ratfish, compared to juveniles, have more pronounced horizontal wear marks (tritors) on their continuously replaced tooth plates (Johnson and Horton, 1972).

Skeletal muscle growth may be mediated by a variety of mechanical inputs (Weijs et al., 1987), but because the twist is restricted to the series elastic element, the observed morphology may be the result of tenocyte reorganization to reduce mechanical shear (Banes et al., 1999; Fong et al., 2005). Twisting the tendon apparently enhances the production of active tension in the muscle but also will mitigate intrafascicular shear by reducing differential strain between different regions of the muscle (van Eijden and Turkawski, 2001). The medial jaw ligaments in elasmobranchs also exhibit a pronounced twist, indicating that this character can apparently form in fibrous tissue in the absence of muscular association (M.N.D., personal observation; C. Wilga, personal communication).

Functional contexts of twisted tendons

We would expect to find a twisted tendon in musculotendon systems with heterogeneous strain distributions where the extreme faces of the muscle exhibit dissimilar external gear ratios (e.g. differential length changes for every angular excursion of the jaws). This will tend to occur in broad muscles (i.e. with proximal and distal faces far apart) attached to rotating structures (i.e. with insertion points that undergo different distance excursions) and inserting far from the joint (i.e. distance excursions/strains are negligible closer to the joint). It is therefore not surprising that the twist is present in the anterior jaw adductor of *H. colliei* but in neither of the more posterior adductors, which insert closer to the jaw joint. Similarly, the lack of twist in the human biceps brachii tendon is consistent with the muscle's narrow breadth and homogeneous moment arm relative to the joint's center of rotation. However, the tendons of both the broad latissimus dorsi and pectoralis major twist before inserting on the humerus in humans, pigs and probably other mammals (Herring et al., 1979; Netter, 2006) (M.N.D., personal observation).

Why are twisted tendons not more ubiquitous in broad muscle systems? Twisted tendons have been recently observed in the mouth closing muscles of several shark species (J. Ramsay, personal communication), but apparently the majority of vertebrate jaw adductors lack twisted tendons, despite having broad origins. We have suggested that in muscles that function to maximize force production, the problem of heterogeneous moment arms must be addressed in order for faces of the muscle to generate maximum force simultaneously. This is impossible in our hypothetical untwisted jaw adductor system where fiber architecture and sarcomere lengths are assumed to be constant. However, if the orientation of the fibers relative to the muscle's line of action varied across the face of the muscle, the regional variation in fiber strains at a given gape may be minimized. It has been shown that architectural variation in different regions of a muscle or between a pair of muscle synergists can function to counteract variation in moment arms and allow for uniform fiber strains (Azizi and Brainerd, 2007). Similarly, if the sarcomere length varies in different regions of a muscle, the differential fiber strains they experience as a result of whole muscle geometry will translate into similar sarcomere strains (Herring et al., 1979; Nordstrom et al., 1974).

Indeed most mammalian adductor muscles (e.g. masseter) have been shown to be heterogeneous with respect to various architectural/functional aspects including fiber architecture and angle (Goto et al., 2001; Turkawski and van Eijden, 2001; van Eijden and Turkawski, 2001; van Eijden et al., 2002). For example, in pigs, rabbits and rats anterior masseter sarcomeres are shorter than posterior ones when the jaw is closed (Herring et al., 1979); as the jaw is opened, fibers across the muscle will tend to strain to similar positions in their length–tension curves

due to the differences in their resting sarcomere lengths. As a result, all sarcomeres may be the same length at a partially opened jaw position (Nordstrom et al., 1974).

We would expect to find force-optimized muscles (broad muscles with twisted tendons or with untwisted tendons and heterogeneous fiber architecture/geometry) in situations where high forces are necessary over a small range of anatomical positions. In a feeding mechanism, this translates to situations where high bite forces are generated over a limited distribution of gape angles, as with prey of a consistent size or the application of prey-cracking force in durophagy. However, in some cases (e.g. more heterogeneous diets), it may be advantageous to generate moderate force over a wider range of anatomical positions (e.g. a diversity of gapes or limb positions). In such situations, we would expect broad muscle architecture similar to our hypothetical untwisted morphology, with homogenous sarcomere lengths, fiber architecture and activation patterns. This ensures that at any anatomical position, some portion of the muscle is generating maximum force and may explain adductor systems with untwisted tendons where resting sarcomere lengths do not differ across the face of the muscle [as in humans (van Eijden et al., 1997)].

In these examples, a trade-off exists between breadth of range of anatomical position and magnitude of force production because muscle fibers are recruited simultaneously. However, in many broad muscles specific regions are recruited independently and represent discrete functional units (compartments). When regional compartmentalization is paired with heterogeneous fiber angle, regions of the muscle can be activated at the joint angle that permits the most efficient transmission of adducting force for that fiber angle (Goto et al., 2001). This may be important for situations necessitating finer control over force production, as in animals with highly heterogeneous diets. A comparable mechanism at the whole muscle level involves dividing the jaw adductor into segregated regions so proximal and distal faces are autonomous units. This is seen in elasmobranchs and derived teleost fishes, which may possess more than ten separate divisions of their adductor mandibulae complexes (Friel and Wainwright, 1999; Korff and Wainwright, 2004; Miyake, 1988).

Apparently, these solutions to moment arm variation are not mutually exclusive and broad muscles may display a complex mosaic of heterogeneities (Turkawski and van Eijden, 2001; van Eijden and Turkawski, 2001; van Eijden et al., 2002). For example, the mammalian latissumus dorsi exhibits the twisted tendon but also functional compartmentalization. Studies of muscle compartmentalization and innervation patterns in mammals suggest a more localized organization of motor control in masticatory muscles as compared to large post-cranial musculature, indicating that a finer gradation of force and movement is possible than in limb or trunk muscles (van Eijden and Turkawski, 2001).

Comparative data on the contractile properties of non-human masticatory motor units is scarce and the small size of jaw adductor muscles in many non-mammalian model organisms makes the accurate determination of compartmentalization more difficult (van Eijden and Turkawski, 2001). Given our current knowledge of the phylogenetic distribution of vertebrate jaw adductor structure and physiology, it appears that compartmentalization and heterogeneous intramuscular fiber architecture are more common in the tetrapod vertebrate condition and that moment arm variation in actinopterygian and chondricthyan fishes is addressed more often through tendon modification (currently known only in chondricthyans) or muscular subdivision (seen in both actinopterygians and chondricthyans). The twisted tendon of the anterior jaw adductor of *H. colliei* represents one potential solution to regional moment arm variation, but may also indicate a lack of intramuscular units. However, we cannot rule out the potential for functional compartmentalization without further studies of *in vivo* function.

Jaw movements represent complex interactions of active and passive muscle tensions and musculotendon form. Feeding musculature with large attachment areas is particularly interesting mechanically and challenging to model for its mosaic of three-dimensional force vectors that share no common origin or insertion. Our analysis of the anterior jaw adductor muscle of *H. colliei* illustrates that simplification of a broad muscle to a single force vector may mask heterogeneities with significance to whole muscle force production. Theoretically, the twisted tendon in this system equalizes strain across the MTC, allowing high force production over a small range of gapes. We therefore hypothesize that this whole muscle modification serves to optimize the muscle not only for active force production but also for distance excursion (i.e. wider gape) by decreasing passive forces resulting from the stretching of the muscle during jaw opening.

Appendix

This geometric model of a hypothetical jaw adductor allows calculation of the lengths of the anterior and posterior faces of a muscle by inputting gape angle and lengths that serve to describe the geometry of the feeding mechanism. The MATLAB code for this model is available to download on M.N.D.'s website. The model (Fig. 3) reduces the system to seven landmarks: anteriormost origin (A), posteriormost origin (B), a point marking the intersection of a line from the jaw joint that is perpendicular to the origin line connecting A and B (C), the jaw joint (D), the posteriormost insertion (E), the anteriormost insertion (F), and a point (G) on a line ($\overline{DG}$) parallel to the origin line and passing through the jaw joint. $\overline{CD}$ is perpendicular to $\overline{DG}$ and $\overline{AB}$. A muscle can therefore be represented schematically as a simple shape comprising four lines: the origin line ($\overline{AB}$), the insertion line ($\overline{EF}$), the anterior muscle face (extending from point A) and the posterior face (extending from point B).

The following measurements were taken from digital photographs of animal specimens: $\overline{CD}$, $\overline{AB}$, $\overline{AC}$, $\overline{DE}$, $\overline{EF}$ and $\angle FDG_0$ (the resting angle of the lower jaw relative to the line $\overline{DG}$; this angle is negative if $\overline{DF}$ is above $\overline{DG}$). From these, the distances from the origin points to the jaw joint and their associated angles were calculated as follows:

$$\overline{AD} = \sqrt{\overline{AC}^2 + \overline{CD}^2} ,$$

$$\overline{BD} = \sqrt{(\overline{AC}+\overline{AB})^2 + \overline{CD}^2} ,$$

$$\angle ADC = \text{atan}(\overline{AC}/\overline{CD}) ,$$

$$\angle BDC = \text{atan}[(\overline{AC}+\overline{AB})/\overline{CD}] .$$

Using these values, it is now possible to calculate the length of the anterior and posterior faces of a muscle using the Law of Cosines. Twisted and untwisted tendons can be thought of as simple modifications to the above geometric model. In an untwisted system, the anterior muscle face inserts on the anterior insertion point (F) and the posterior face on the posterior insertion point (E), while in the twisted system the anterior and posterior faces exchange their insertion points and insert at E and F, respectively. As a result, the anterior and posterior faces are depicted by $\overline{AF}$ and $\overline{BE}$ in the untwisted system and by $\overline{AE}$ and $\overline{BF}$ in the twisted model, the lengths of which are calculated as follows:

Untwisted model

Anterior face:

$$\overline{AF} = \sqrt{\overline{AD}^2 + \overline{FD}^2 - 2\overline{AD} \times \overline{FD} \times \cos\angle ADE} ,$$

where $\angle ADE = \angle ADC + 90° + \angle FDG_0 + X°$ and X°=angular difference from resting angle (e.g. with mouth closed, X=0° and with a 40° gape, X=40°).

Posterior face:

$$\overline{BE} = \sqrt{\overline{BD}^2 + \overline{ED}^2 - 2\overline{BD} \times \overline{ED} \times \cos\angle BDE} ,$$

where $\angle BDE = \angle BDC + 90° + \angle FDG_0 + X°$.

Twisted model

Anterior face:

$$\overline{AE} = \sqrt{\overline{AD}^2 + \overline{ED}^2 - 2\overline{AD} \times \overline{ED} \times \cos\angle ADE} ,$$

Posterior face:

$$\overline{BF} = \sqrt{\overline{BD}^2 + \overline{FD}^2 - 2\overline{BD} \times \overline{FD} \times \cos\angle BDE} ,$$

where $\angle ADE$ and $\angle BDE$ are calculated as above.

Since the distance of the attachment points from the jaw joint will not change with gape angle (Figs 1, 3), this same model can be used to determine muscle length at any gape angle, simply by adjusting the angle term, X°.

For each gape angle in question and for twisted and untwisted conditions, we calculated the percentage length change (strain) for each muscular face by dividing the difference between the current length and resting length by the resting length ($L–L_r/L_r$). In lateral view, the length of the MTC is at the least only 23.0% muscle and no more than 27% muscle; therefore strains calculated relative to the entire complex are overestimates. We accounted for this by multiplying the MTC resting length by 0.245 to more accurately represent the resting length over which the stretching is occurring:

$$\text{Untwisted (anterior face strain)} = (\overline{AF}_X – \overline{AF}_0) / (0.245 \times \overline{AF}_0) ,$$

$$\text{Untwisted (posterior face strain)} = (\overline{BE}_X – \overline{BE}_0) / (0.245 \times \overline{BE}_0) ,$$

$$\text{Twisted (anterior face strain)} = (\overline{AE}_X – \overline{AE}_0) / (0.245 \times \overline{AE}_0) ,$$

$$\text{Twisted (posterior face strain)} = (\overline{BF}_X – \overline{BF}_0) / (0.245 \times \overline{BF}_0) .$$

Our analysis treats the two faces of the muscle as extremes in the system. We compare twisted and untwisted morphologies by memorializing the strain field of each muscle as the difference between the strains of the two faces (ΔS=anterior face strain–posterior face strain). A ΔS value of zero represents uniform strain in the muscle and positive and negative values indicate relatively higher and lower anterior face strains, respectively (Fig. 4).

This model operates under several simplifying assumptions, also used in other studies to characterize muscle geometry and infer function (e.g. Goto et al., 2001; Herring et al., 1979; Peck et al., 2000; van der Helm and Veenbaas, 1991). We assume anterior and posterior face fibers are of similar fiber type and undergo similar deformations during mouth opening, that fascicle strain regimes do not vary significantly in different regions of the muscle. We assume that recruitment is constant across the two faces of the muscle and that there is no compartmentalization of function during feeding. Although adjacent fibers and fiber bundles can be connected *via* connective tissue attachments, we treat interfiber interactions as negligible. Fascicle strain across the muscle is calculated at the two anterior and posterior ends of the muscle and assumed to be a gradient between these regions (Goto et al., 2001; van Eijden and Koolstra, 1998). We ignore any compliance of the tendon, which may partly decouple fascicle shortening from shortening of the whole MTC; however, this assumption is not expected to have large effects on our predicted fiber strains (Goto et al., 2001; Lichtwark and Wilson, 2006). Finally, since our observations indicate that the tendon fibers are largely linearly arrayed, we assume that muscle forces are only transferred directly to the mandible *via* the specific region of the tendon to which the fascicles attach. The consequences for violations of these assumptions are addressed in the Discussion.

In a lever system such as the jaw of *H. colliei*, output force (bite force, F_o) is a function of input force (muscle force, F_i), input lever arm (l_i) and output lever arm (l_o):

$$F_o = F_i l_i / l_o .$$

In our geometric model, the anterior and posterior borders of the MTC summarize the AMA-α by localizing the anteriormost and posteriormost origin and insertion points. Since the twisted and untwisted conditions modeled above share the same origin and insertion points (although the anterior face inserts on the posterior insertion point in the twisted condition and the anterior insertion point in the untwisted condition, etc.) and bite force can be assumed to be applied at the toothplates in both cases, the input and output lever arms are the same between the two conditions. As such, bite force can be compared between the two conditions by investigating differences in the orientation of the input force vector.

The proportion of muscle contractile force transferred to the insertion element is a function of the angle of insertion of the muscle fibers and can be expressed by multiplying contractile force by the sine of the insertion angle. As such, only a fiber that inserts at a right angle to the jaw will exert its full force potential (100%) in a direction normal to the insertion element, whereas a fiber inserting at 50° exerts only 76.6% of its generated force.

Our model does not provide bite force estimates; however, if we assume that the anterior and posterior margins of the MTC generate similar forces in both conditions, we can hypothesize effective force transmission by calculating the magnitude of the component input force normal to the jaw and parallel to the bite force vector. We can then investigate the effect and potential

trade-offs of a twisted tendon (i.e. shallower insertion angles) on effective force production by comparing the sine of the insertion angles for anterior and posterior faces in both twisted and untwisted conditions.

Insertion angle was calculated by the Law of Cosines using distances determined for the basic model above:

Untwisted (anterior face insertion):

$$\angle \mathrm{AFD} = \mathrm{acos}\left(\frac{\overline{\mathrm{FD}}^2+\overline{\mathrm{AF}}^2-\overline{\mathrm{AD}}^2}{2\times\overline{\mathrm{FD}}\times\overline{\mathrm{AF}}}\right),$$

Untwisted (posterior face insertion):

$$\angle \mathrm{BED} = \mathrm{acos}\left(\frac{\overline{\mathrm{ED}}^2+\overline{\mathrm{BE}}^2-\overline{\mathrm{BD}}^2}{2\times\overline{\mathrm{ED}}\times\overline{\mathrm{BE}}}\right),$$

Twisted (posterior face insertion):

$$\angle \mathrm{AED} = \mathrm{acos}\left(\frac{\overline{\mathrm{ED}}^2+\overline{\mathrm{AE}}^2-\overline{\mathrm{AD}}^2}{2\times\overline{\mathrm{ED}}\times\overline{\mathrm{AE}}}\right),$$

Twisted (posterior face insertion):

$$\angle \mathrm{BFD} = \mathrm{acos}\left(\frac{\overline{\mathrm{FD}}^2+\overline{\mathrm{BF}}^2-\overline{\mathrm{BD}}^2}{2\times\overline{\mathrm{FD}}\times\overline{\mathrm{BF}}}\right).$$

The calculations take into account the slope of the insertion line (i.e. $\overline{\mathrm{DF}}$, the lower jaw) allowing us to determine the change in all four insertion angles at any gape angle. We graphically compared the sines of these angles across the natural gape cycle (0–40°) to illustrate the effect of a twisted tendon (i.e. shallower insertion angles) on the component of contractile force in the direction of bite force (Fig. 5).

We would like to thank Beth Brainerd, Dave Carrier, Tom Koob and the UCI Biomechanics Lab for helpful comments on this manuscript. Cindy Klepadlo and H. J. Walker at the Scripps Museum generously furnished the ontogenetic series of specimens. Nate Kley, Robert Leonard, Hans Hoeppler, Jason Ramsay and Cheryl Wilga supplied encouragement and examples of twisted tendons in other taxa. Animal use in this study complied with the policies espoused by the University of Washington Institutional Animal Care and Use Committee. This work was funded under a National Science Foundation grant to M.N.D. and A.P.S. (IOB-0616322), and GAAN, Frances Benton and Chancellor's Club fellowships to M.N.D.

References

Azizi, E. and Brainerd, E. (2007). Architectural gear ratio and strain homogeneity in segmented musculature. *J. Exp. Zool. Part A* **134**, 145-155.

Banes, A. J., Horesovsky, G., Larson, C., Tsuzaki, M., Judex, S., Archambault, J., Zernicke, R., Herzog, W., Kelley, S. and Miller, L. (1999). Mechanical load stimulates expression of novel genes in vivo and in vitro in avian flexor tendon cells. *Osteoarthr. Cartil.* **7**, 141-153.

Didier, D. A. (1995). Phylogenetic systematics of the extant chimaeroid fishes (Holocephali, Chimaeroidei). *Am. Mus. Novit.* **3119**, 1-86.

Ebert, D. A. (2003). *Sharks, Rays and Chimaeras of California*. Berkeley: University of California Press.

Fong, K. D., Trindade, M. C., Wang, Z., Nacamuli, R. P., Pham, H., Fang, T. D., Song, H. J. M., Smith, L., Longaker, M. T. and Chang, J. (2005). Microarray analysis of mechanical shear effects on flexor tendon cells. *Plast. Reconstr. Surg.* **116**, 1393-1404.

Friel, J. P. and Wainwright, P. C. (1999). Evolution of complexity in motor patterns and jaw musculature of tetraodontiform fishes. *J. Exp. Biol.* **202**, 867-880.

Gillis, G. B., Flynn, J. P., McGuigan, P. and Biewener, A. A. (2005). Patterns of strain and activation in the thigh muscles of goats across gaits during level locomotion. *J. Exp. Biol.* **208**, 4599-4611.

Gordon, A. M., Huxley, A. F. and Julian, F. J. (1966). The variation in isometric tension with sarcomere length in vertebrate muscle fibers. *J. Physiol.* **184**, 170-192.

Goto, T. K., Langenbach, G. E. J. and Hannam, A. G. (2001). Length changes in the human masseter muscle after jaw movement. *Anat. Rec.* **262**, 293-300.

Hernandez, L. P. and Motta, P. J. (1997). Trophic consequences of differential performance: ontogeny of oral jaw-crushing performance in the sheepshead, *Archosargus probatocephalus* (Teleostei, Sparidae). *J. Zool. Lond.* **243**, 737-756.

Herring, S. W., Grimm, A. F. and Grimm, B. R. (1979). Functional heterogeneity in a multipinnate muscle. *Am. J. Anat.* **154**, 563-575.

Huber, D. R., Dean, M. N. and Summers, A. P. (2004). The crushing bite of the water bunny. *Integr. Comp. Biol.* **44**, 573.

Johnson, A. G. and Horton, H. F. (1972). Length-weight relationship, food habits, parasites, and sex and age determination of the ratfish, *Hydrolagus colliei* (Lay and Bennett). *Fish. Bull.* **70**, 421-429.

Koolstra, J. H. and van Eijden, T. M. G. (1997). Dynamics of the human masticatory muscles during a jaw open-close movement. *J. Biomech.* **30**, 883-889.

Korff, W. L. and Wainwright, P. C. (2004). Motor pattern control for increasing crushing force in the striped burrfish (*Chilomycterus schoepfi*). *Zoology* **107**, 335-346.

Lichtwark, G. A. and Wilson, A. M. (2006). Interactions between the human gastrocnemius muscle and the Achilles tendon during incline, level and decline locomotion. *J. Exp. Biol.* **209**, 4379-4388.

Miyake, T. (1988). The systematics of the stingray genus *Urotrygon* with comments on the interrelationships within Urolophidae (Chondrichthyes, Myliobatiformes). PhD thesis, Texas A&M University, College Station, Texas, USA.

Netter, F. H. (2006). *Atlas of Human Anatomy*. St Louis: W. B. Saunders.

Nordstrom, S. H. and Yemm, R. (1974). Relationship between jaw position and isometric active tension produced by direct stimulation of rat masseter muscle. *Arch. Oral Biol.* **19**, 353-359.

Nordstrom, S. H., Bishop, M. and Yemm, R. (1974). Effect of jaw opening on sarcomere length of the masseter and temporal muscles of the rat. *Arch. Oral Biol.* **19**, 151-155.

Pappas, G. P., Asakawa, D. S., Delp, S. L., Zajac, F. E. and Drace, J. E. (2002). Nonuniform shortening in the biceps brachii during elbow flexion. *J. Appl. Physiol.* **92**, 2381-2389.

Peck, C. C., Langenbach, G. E. J. and Hannam, A. G. (2000). Dynamic simulation of muscle and articular properties during human wide jaw opening. *Arch. Oral Biol.* **45**, 963-982.

Turkawski, S. J. J. and van Eijden, T. M. G. J. (2001). Mechanical properties of single motor units in the rabbit masseter muscle as a function of jaw position. *Exp. Brain Res.* **138**, 153-162.

van der Helm, F. C. T. and Veenbaas, R. (1991). Modeling the mechanical effect of muscles with large attachment sites: Application to the shoulder mechanism. *J. Biomech.* **24**, 1151-1163.

van Eijden, T. M. G. J. and Koolstra, J. H. (1998). A model for mylohyoid muscle mechanics. *J. Biomech.* **31**, 1017-1024.

van Eijden, T. M. G. J. and Turkawski, S. J. J. (2001). Morphology and physiology of masticatory muscle motor units. *Crit. Rev. Oral Biol. Med.* **12**, 76-91.

van Eijden, T. M. G. J., Korfage, J. A. M. and Brugman, P. (1997). Architecture of the human jaw-closing and jaw-opening muscles. *Anat. Rec.* **248**, 464-474.

van Eijden, T. M. G. J., Turkawski, S. J. J., van Ruijven, L. J. and Brugman, P. (2002). Passive force characteristics of an architecturally complex muscle. *J. Biomech.* **35**, 1183-1189.

Wainwright, P. C. (1987). Biomechanical limits to ecological performance: mollusc-crushing by the Caribbean hogfish, *Lachnolaimus maximus* (Labridae). *J. Zool. Lond.* **213**, 283-297.

Weijs, W. A., Brugman, P. and Klok, E. M. (1987). The growth of the skull and jaw muscles and its functional consequences in the New Zealand rabbit (*Oryctolagus cuniculus*). *J. Morphol.* **194**, 143-161.

Winter, D. A. (1990). Muscle mechanics. In *Biomechanics and Motor Control of Human Movement*, pp. 165-189. New York: John Wiley & Sons.

Woittiez, R. D., Huijing, P. A. and Rozendal, R. H. (1983). Influence of muscle architecture on the length-force diagram of mammalian muscle. *Pflügers Arch.* **399**, 275-279.